Progress In Electromagnetics Research Letters, Vol. 62, 29–34, 2016

Quasi-static Vertical Magnetic Field of a Large Horizontal Circular Loop Located at the Earth's Surface

Mauro Parise*

Abstract—In this work, an analytical expression is derived for the radial distribution of the quasi-static vertical magnetic field of a current-carrying large circular loop placed on a homogeneous earth. The obtained expression results from applying a rigorous procedure, which leads to cast the Hankel transform describing the vertical magnetic field component into a form consisting of two elliptic integrals and a fast-convergent sum of spherical Hankel functions. The derived solution ensures the same degree of accuracy as the finite difference time domain method, but, as a purely analytical formula, has the advantage of requiring less computational time. Numerical results are presented to illustrate the validity of the developed formulation.

1. INTRODUCTION

In the last decades, the problem of evaluating the electromagnetic field distribution of a current-carrying loop placed in close proximity to a homogeneous dispersive medium has attracted the interest of researchers working in a number of scientific fields, including radio communication, radio remote sensing, and diathermy [1–12]. For instance, accurate field computation is important in geophysical applications, since comparison of the theoretical and measured vertical magnetic field produced by a close-to-the-surface loop antenna permits to detect shallow buried objects like mines, metals, mineral resources or other ground inhomogeneities [1, 4, 10]. In spite of the relevance of the problem, to date analytical expressions for the spatial distributions of the generated fields still are not available. Thus, the problem of a horizontal loop lying on a homogeneous ground is typically solved through numerical procedures, which may consist of either integration techniques for evaluating the integral representations for the fields (like Gaussian quadrature), or simulation tools for solving general electromagnetic boundary value problems, like the finite difference time domain (FDTD) method [1]. Both techniques present drawbacks. Numerical integration is made difficult and impractical by the highly oscillatory nature of the integrals describing the fields, while tools like the FDTD method are subject to numerical dispersion errors [8]. In an attempt to overcome the drawbacks of numerical techniques, some authors [13] recently proposed a hybrid analytical-numerical approach for evaluating the field integrals, based on performing analytical integration after replacing part of the integrand with a suitable rational function generated by Newton's iterative method. This approach has been shown to lead to highly accurate results, but has the disadvantage to provide field expressions which are not completely analytical, but contain a large set of numerical coefficients whose computation is time-consuming [13].

The present work introduces a procedure that allows to analytically evaluate the Hankel transform describing the radial distribution of the quasi-static vertical magnetic field of a circular loop antenna lying on the surface of a lossy earth structure. The procedure makes it possible to cast the field integral into a form involving only two elliptic integrals and a fast-convergent sum of spherical Hankel functions. Such a purely analytical solution permits to avoid usage of standard numerical procedures as

Received 30 May 2016, Accepted 26 August 2016, Scheduled 2 September 2016
* Corresponding author: Mauro Parise (m.parise@unicampus.it).
The author is with the Faculty of Engineering, University Campus Bio-Medico of Rome, Rome 00128, Italy.

well as the previously published quasi-analytical expression for the magnetic field of the loop [13]. The derived formulation is also of practical use as an analytical benchmark for simulation tools employed to solve electromagnetic boundary value problems, with applications in antenna design and radio communication.

The validity of the proposed solution is demonstrated in Section 3, where it is used to compute profiles of the amplitude of the vertical magnetic field against frequency and source-receiver distance. The achieved results are seen to be in excellent agreement with the data from FDTD simulations.

2. FORMULATION

Consider a current-carrying horizontal circular loop lying on the surface of a homogeneous lossy ground, as shown in Fig. 1. The emitter carries a uniform current equal to $Ie^{j\omega t}$. The dielectric permittivity and electric conductivity of the medium are denoted by ϵ_1 and σ_1, respectively, while the magnetic permeability is assumed to be everywhere that of free-space. In the quasi-static limit, that is when the source-receiver distance is much smaller than the free-space wavelength ($k_0\rho \ll 1$), the H_z-field generated by the loop in the air space is described by the Hankel transform [8]

$$H_z = -Ia\frac{1}{\rho}\frac{\partial}{\partial\rho}\left(\rho\frac{\partial}{\partial\rho}\int_0^\infty \frac{e^{-\lambda z}}{\lambda+u}J_0(\lambda\rho)J_1(\lambda a)d\lambda\right), \tag{1}$$

being $J_n(\cdot)$ the nth-order Bessel function, and

$$u = \sqrt{\lambda^2 - k_1^2}, \quad \mathrm{Re}[u]>0, \tag{2}$$

$$k_1^2 = -j\omega\mu_0\left(\sigma_1 + j\omega\epsilon_1\right). \tag{3}$$

The aim of this work is to evaluate Eq. (1) at the air-ground interface ($z=0^+$). To this end, we first multiply the numerator and denominator of the integrand by $(\lambda - u)$, so as to express the field integral as

$$H_{z0} = \frac{Ia}{k_1^2\rho}\frac{\partial\left[\rho\left(P_1+P_2\right)\right]}{\partial\rho}, \tag{4}$$

where the subscript 0 denotes calculation at $z=0^+$, and

$$P_1 = -\left[\frac{\partial}{\partial\rho}\int_0^\infty \lambda e^{-\lambda z}J_0(\lambda\rho)J_1(\lambda a)d\lambda\right]_{z=0^+}, \tag{5}$$

$$P_2 = \left[\frac{\partial}{\partial\rho}\int_0^\infty u e^{-\lambda z}J_0(\lambda\rho)J_1(\lambda a)d\lambda\right]_{z=0^+}. \tag{6}$$

Notice that P_1 and P_2 are, respectively, above-surface ground wave and lateral wave terms [14]. Next, use of the identity [16]

$$\lambda J_1(\lambda a) = -\frac{\partial J_0(\lambda a)}{\partial a} \tag{7}$$

allows to turn Eq. (5) into the expression

$$P_1 = \frac{\partial^2}{\partial\rho\partial a}\int_0^\infty J_0(\lambda\rho)J_0(\lambda a)d\lambda, \tag{8}$$

the integral on the right-hand side of which is tabulated in [3]. It reads

$$\int_0^\infty J_0(\lambda\rho)J_0(\lambda a)d\lambda = \frac{2}{\pi\left(a+\rho\right)}K\left(\frac{2\sqrt{a\rho}}{a+\rho}\right), \tag{9}$$

where

$$K(\xi) = \int_0^{\frac{\pi}{2}}\left(1-\xi^2\sin^2\phi\right)^{-1/2}d\phi \tag{10}$$

is the complete elliptic integral of the first kind. Differentiating Eq. (9) with respect to ρ and a leads to the explicit form of the ground-wave term P_1, namely

$$P_1 = \frac{1}{\pi a\rho\,(a+\rho)}\left[\frac{\rho^2+a^2}{(a-\rho)^2}E\left(\frac{2\sqrt{a\rho}}{a+\rho}\right) - K\left(\frac{2\sqrt{a\rho}}{a+\rho}\right)\right], \tag{11}$$

where

$$E(\xi) = \int_0^{\frac{\pi}{2}} \left(1-\xi^2\sin^2\phi\right)^{1/2} d\phi \tag{12}$$

is the complete elliptic integral of the second kind. On the other hand, to evaluate Eq. (6) it suffices to move the ρ-derivative under the integral sign, as follows

$$P_2 = -\left[\int_0^{\infty} ue^{-\lambda z}J_1(\lambda\rho)J_1(\lambda a)\lambda d\lambda\right]_{z=0^+}, \tag{13}$$

and, after setting z=0, perform the replacement

$$u = \left[\frac{\partial^2}{\partial\zeta^2}\left(\frac{e^{-u\zeta}}{u}\right)\right]_{\zeta=0} \tag{14}$$

so as to obtain

$$P_2 = -\left[\frac{\partial^2}{\partial\zeta^2}\int_0^{\infty}\frac{e^{-u\zeta}}{u}J_1(\lambda\rho)J_1(\lambda a)\lambda d\lambda\right]_{\zeta=0}. \tag{15}$$

Next, after substituting the identity [15]

$$J_1(\lambda\rho)J_1(\lambda a) = \frac{1}{\pi}\int_0^{\pi} J_0\left(\lambda R'\right)\cos\phi d\phi, \tag{16}$$

where

$$R' = \sqrt{\rho^2+a^2-2a\rho\cos\phi} = \sqrt{R^2-2a\rho\cos\phi}, \tag{17}$$

interchange of the order of the integrals and use of the well known result

$$\int_0^{\infty}\frac{e^{-u\zeta}}{u}J_0\left(\lambda R'\right)\lambda d\lambda = \frac{e^{-jk_1R''}}{R''}, \tag{18}$$

with

$$R'' = \sqrt{R^2+\zeta^2-2a\rho\cos\phi}, \tag{19}$$

allows to convert Eq. (15) into

$$P_2 = -\frac{1}{\pi}\left[\frac{\partial^2}{\partial\zeta^2}\int_0^{\pi}\frac{e^{-jk_1R''}}{R''}\cos\phi d\phi\right]_{\zeta=0}. \tag{20}$$

The integral on the right-hand side of Eq. (20) may be expressed as an infinite sum of spherical Hankel functions of the second kind [9]. It reads

$$\int_0^{\pi}\frac{e^{-jk_1R''}}{R''}\cos\phi d\phi = -j\pi k_1\sum_{l=1}^{\infty}\frac{\left(k_1^2a\rho/2\right)^{2l-1}}{l!(l-1)!}\frac{h_{2l-1}^{(2)}(k_1\tilde{R})}{(k_1\tilde{R})^{2l-1}}, \tag{21}$$

being $\tilde{R} = \sqrt{R^2+\zeta^2}$, and, as a consequence, the lateral-wave term P_2 becomes

$$P_2 = jk_1\sum_{l=1}^{\infty}\frac{\left(k_1^2a\rho/2\right)^{2l-1}}{l!(l-1)!}\left[\frac{\partial^2}{\partial\zeta^2}\frac{h_{2l-1}^{(2)}(k_1\tilde{R})}{(k_1\tilde{R})^{2l-1}}\right]_{\zeta=0} = -jk_1^3\sum_{l=1}^{\infty}\frac{\left(k_1^2a\rho/2\right)^{2l-1}}{l!(l-1)!}\frac{h_{2l}^{(2)}(k_1R)}{(k_1R)^{2l}}. \tag{22}$$

Finally, combining Eqs. (11) and (22) with Eq. (1), and performing the ρ-derivative, provides the formula

$$\begin{aligned} H_{z0} \;=\; & \frac{I}{\pi k_1^2\,(a-\rho)\,(a+\rho)^2}\left[\frac{7a^2+\rho^2}{(a-\rho)^2}E\left(\frac{2\sqrt{a\rho}}{a+\rho}\right) - K\left(\frac{2\sqrt{a\rho}}{a+\rho}\right)\right] \\ & + jk_1^3a^2I\sum_{l=1}^{\infty}\frac{\left(k_1^2a\rho/2\right)^{2l-2}}{[(l-1)!]^2}\left[\frac{(k_1\rho)^2}{2l}\frac{h_{2l+1}^{(2)}(k_1R)}{(k_1R)^{2l+1}} - \frac{h_{2l}^{(2)}(k_1R)}{(k_1R)^{2l}}\right]. \end{aligned} \tag{23}$$

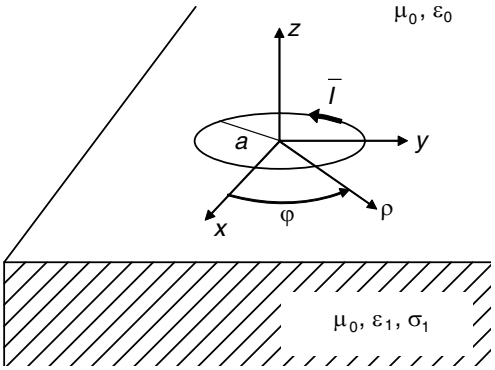

Figure 1. Sketch of a circular loop antenna on a homogeneous ground.

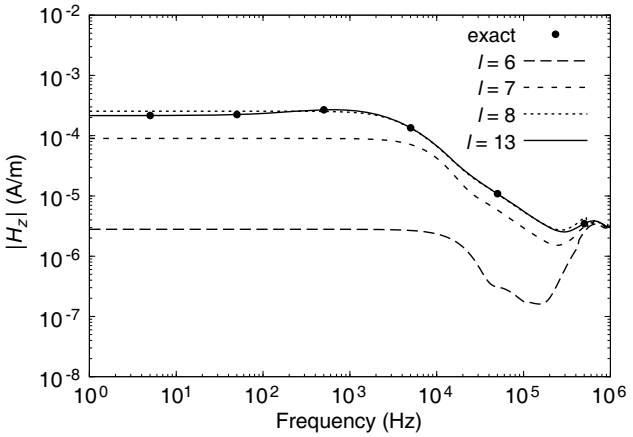

Figure 2. Amplitude-frequency spectrum of H_z, computed at ρ=40 m from the loop axis.

3. RESULTS AND DISCUSSION

To check the accuracy of the presented approach, expression (23) is applied to the computation of the time-harmonic H_z-field produced on the top surface of a homogeneous medium at distance ρ=40 m from a circular loop, 20 m in radius, which carries 1 A of current. The electrical conductivity and dielectric permittivity of the medium are σ_1=10 mS/m and ϵ_1=5ϵ_0, respectively, and frequency is assumed to range between 1 Hz and 1 MHz, where the quasi-static condition $k_0\rho \ll 1$ is met. The calculations are performed on a 2.33 GHz Intel Xeon e5345 processor, and the obtained results, depicted in Figs. 2 and 3, are compared with those resulting from FDTD simulations. The three-dimensional FDTD mesh is configured with $300 \times 300 \times 6$ cubic cells of size 25 cm, spanning a computational volume of $75 \times 75 \times 1.5$ m centered at the origin. The grid is terminated by the PMLs in all three directions of the Cartesian coordinate system. Fig. 2 shows the behavior of the frequency spectrum of $|H_z|$ as the number of terms of the sum of spherical hankel functions in Eq. (23) is increased. What emerges is that convergence of the sum is fast, since 13 terms are enough to achieve a curve that perfectly matches the exact FDTD data, denoted by points.

On the other hand, as the accuracy of the solution depends on the convergence of the infinite sum, it is concluded that the contribution of the lateral wave field to the total field is not negligible. This aspect is pointed out in Fig. 3, which illustrates the above-ground and lateral-wave fields produced by the circular loop source in the quasi-static frequency range. The upper subfigure also shows the total field resulting from the two contributions. Again, computations have been performed truncating the infinite sum in (23) at l=13. A glance at the curves plotted in Fig. 3 reveals that the ground and lateral waves interfere destructively, and that the destructive effect of the lateral wave becomes more and more important as frequency decreases. At extremely low frequencies, the lateral wave has the effect of reducing the vertical magnetic field by about three orders of magnitude.

As previously observed, the proposed formula ensures the same degree of accuracy as the FDTD

Table 1. Speed-up in computation time offered by the proposed formula over FDTD method.

Approach	Time consumption (s)	Speed-up	RMS rel. error (%)
New (300×300)	94.2	1	0
3D FDTD ($50 \times 50 \times 1$)	32.3	0.34	12.11
3D FDTD ($100 \times 100 \times 2$)	144.8	1.54	6.42
3D FDTD ($300 \times 300 \times 6$)	2831.7	30.06	0.28

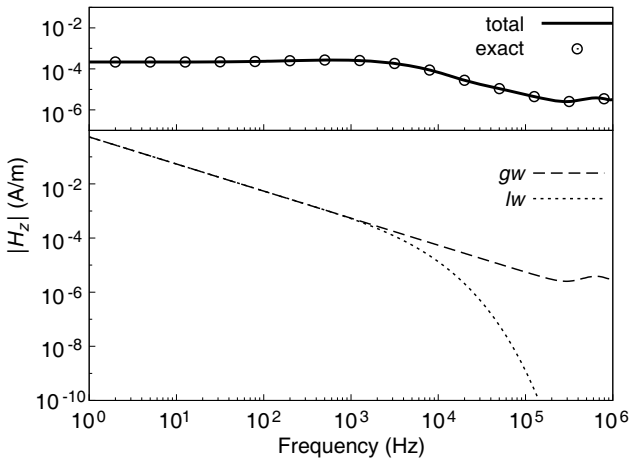

Figure 3. Amplitude-frequency spectra of ground wave (gw), lateral wave (lw), and total vertical magnetic field generated by the loop source, computed at ρ=40 m from the loop axis.

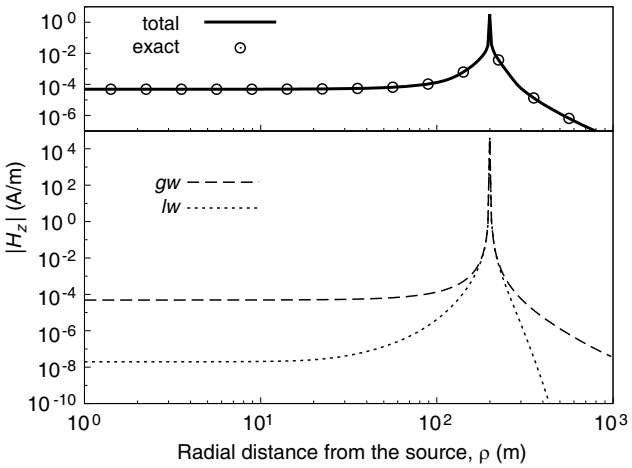

Figure 4. Radial distributions of the magnitudes of ground wave (gw), lateral wave (lw), and total vertical magnetic field generated by the loop source, computed at the frequency of 10 kHz.

method. One would ask which of the approaches is less time consuming. This comparison is illustrated in Table 1, which shows the computation time for the each method, that is the time taken to compute the vertical magnetic field at the observation grid points lying on the 75×75 m square centered at the origin. The loop is assumed to operate at the frequency of 10 kHz. Table 1 also depicts the ratio of the time taken by the FDTD scheme to that required by (23), that is the gain in computation time (speed-up). It can be noticed that, accuracy being equal, the speed-up offered by (23) is about 30. Conversely, the FDTD procedure may become faster than the proposed approach, but only at the price of using a coarse mesh ($50 \times 50 \times 1$), which cannot give rise to accurate results. This is confirmed by the entries in the fourth column of Table 1, which contain the root-mean-square (RMS) relative errors that result from calculating the H_z-field of the loop by using the FDTD method rather than the proposed field expression. The mean is taken over the set of grid points on the 75×75 m square centered at the origin. Finally, Fig. 4 shows the amplitude of H_z against the source-receiver distance ρ. The calculations have been performed assuming that the loop source, 200 m in radius, is positioned on the same medium as in the previous examples, and that it still operates at 10 kHz. As seen, the profiles of the ground and lateral wave fields are similar, and both exhibit an in-loop region, where the field weakly depends on ρ, and an offset loop region, where the field rapidly decays with increasing ρ. In particular, the ground wave predominates over the lateral wave at all the field points, except in close proximity to the edge of the loop, where they almost cancel out.

4. CONCLUSION

The aim of this work is to present an analytical expression that allows to accurately calculate the radial distribution of the quasi-static vertical magnetic field generated by a large circular loop located on a homogeneous ground. The derived expression consists of two elliptic integrals plus a fast-convergent sum of spherical Hankel functions and has the advantage of requiring less computational time than standard simulation tools for solving boundary value problems, as the FDTD method.

REFERENCES

1. Zhdanov, M. S., *Geophysical Electromagnetic Theory and Methods*, Elsevier, Amsterdam, 2009.
2. Parise, M., "Exact electromagnetic field excited by a vertical magnetic dipole on the surface of a lossy half-space," *Progress In Electromagnetics Research B*, Vol. 23, 69–82, 2010.

3. Parise, M., "An exact series representation for the EM field from a circular loop antenna on a lossy half-space," *IEEE Antennas and Wireless Prop. Letters*, Vol. 13, 23–26, 2014.
4. Parise, M., "Fast computation of the forward solution in controlled-source electromagnetic sounding problems," *Progress In Electromagnetics Research*, Vol. 111, 119–139, 2011.
5. Kong, J. A., *Electromagnetic Wave Theory*, John Wiley & Sons, New York, 1986.
6. Chew, W. C., *Waves and Fields in Inhomogeneous Media*, Van Nostrand Reinhold, New York, 1990.
7. Singh, N. P. and T. Mogi, "Electromagnetic response of a large circular loop source on a layered earth: A new computation method," *Pure and Applied Geophysics*, Vol. 162, No. 1, 181–200, 2005.
8. Ward, S. H. and G. W. Hohmann, "Electromagnetic theory for geophysical applications," *Electromagnetic Methods in Applied Geophysics, Theory*, Vol. 1, 131–308, edited by M. N. Nabighian, SEG, Tulsa, Oklahoma, 1988.
9. Werner, D. H., "An exact integration procedure for vector potentials of thin circular loop antennas," *IEEE Transactions on Antennas and Propagation*, Vol. 44, 157–165, 1996.
10. Palacky, G. J., "Resistivity characteristics of geologic targets," *Electromagnetic Methods in Applied Geophysics*, Vol. 1, 52–129, M. N. Nabighian, Ed., SEG, Tulsa, Oklahoma, 1988.
11. Parise, M. and S. Cristina, "High-order electromagnetic modeling of shortwave inductive diathermy effects," *Progress In Electromagnetics Research*, Vol. 92, 235–253, 2009.
12. Parise, M., "On the use of cloverleaf coils to induce therapeutic heating in tissues," *Journal of Electromagnetic Waves and Applications*, Vol. 25, Nos. 11–12, 1667–1677, 2011.
13. Parise, M., "A study on energetic efficiency of coil antennas used for RF diathermy," *IEEE Antennas and Wireless Prop. Letters*, Vol. 10, 385–388, 2011.
14. Parise, M., "An exact series representation for the EM field from a vertical electric dipole on an imperfectly conducting half-space," *Journal of Electromagnetic Waves and Applications*, Vol. 28, No. 8, 932–942, 2014.
15. Erdelyi, A., *Tables of Integral Transforms*, Vol. 2, McGraw-Hill, New York, 1954.
16. Abramowitz, M. and I. A. Stegun, *Handbook of Mathematical Functions with Formulas, Graphs, and Mathematical Tables*, Dover, New York, 1964.